Terrigenous plant wax inputs to the Arabian Sea: Implications for the reconstruction of winds associated with the Indian Monsoon

Kristina A. Dahl[*1], Delia W. Oppo[2], Timothy I. Eglinton[3],

Konrad A. Hughen[3], William B. Curry[2], and Frank Sirocko[4]

[*] Corresponding author

[1]MIT/WHOI Joint Program, Woods Hole Oceanographic Institution

WHOI MS #22, Woods Hole, MA 02543 USA. kdahl@whoi.edu

[2]Department of Marine Geology and Geophysics, Woods Hole Oceanographic Institution, USA

[3]Department of Marine Chemistry and Geochemistry, Woods Hole Oceanographic Institution, USA

[4]Institut für Geowissenchaften, J. Gutenberg Universität Mainz, Mainz, Germany

Abstract

We have determined the accumulation rates and carbon isotopic compositions (δ^{13}C) of long–chain (C_{24}–C_{32}) terrigenous plant wax fatty acids in 19 surface sediment samples geographically distributed throughout the Arabian Sea in order to assess the relationship between plant wax inputs and the surrounding monsoon wind systems. Both the accumulation rate data and the δ^{13}C data show that there are three primary eolian sources of plant waxes to the Arabian Sea: Africa, Asia, and the Arabian Peninsula. These sources correspond to the three major wind systems in this region: the summer (Southwest) monsoon, the winter (Northeast) monsoon, and the summer northwesterlies that blow over the Arabian Peninsula. In addition, plant waxes are fluvially supplied to the Gulf of Oman and the Eastern African margin by nearby rivers. Plant wax δ^{13}C values reflect the vegetation types of the continental source regions. Greater than 75% of the waxes from Africa and Asia are derived from C_4 plants. Waxes delivered by northwesterly winds reflect a greater influence (25–40%) of C_3 vegetation, likely derived from the Mesopotamian region. These data agree well with previously published studies of eolian dust deposition, particularly of dolomite derived from the Arabian Peninsula and the Mesopotamian region, in surface sediments of the Arabian Sea. The west–to–east gradient of plant wax δ^{13}C and dolomite accumulation rates are separately useful indicators of the relationship between the northwesterly winds and the winds of the Southwest monsoon. Combined, however, these two proxies could provide a powerful tool for the reconstruction of both southwest monsoon strength as well as Mesopotamian aridity.

1 INTRODUCTION

The Asian monsoon system is one of the most important components of Earth's climate today because of its broad influence in both tropical and extratropical regions. With over 60% of the

planet's population living within monsoon–affected regions, it is critical that we develop an understanding of not only present–day monsoon climatology, but also potential monsoonal variability by studying the past. This study aims to assess the potential of terrestrial plant waxes as recorders of wind source and strength for winds associated with the Indian Monsoon. This is accomplished by mapping the accumulation rate and carbon isotopic composition (δ^{13}C) of plant waxes in surface sediments from throughout the Arabian Sea.

The Indian monsoon system is associated with strong winds that have the potential to carry large amounts of terrestrial material to the Arabian Sea from the surrounding land masses. Seasonal changes in wind direction (Figure 1), and therefore source region for eolian material, produce a mixture of components that are integrated into the sediment record. During boreal summer, southwesterly winds (up to 30 $m\ s^{-1}$) associated with the summer monsoon blow over Ethiopia and Somalia, potentially carrying material from Africa to the Arabian Sea (Ramage et al., 1972). These summer monsoon winds are driven a gradient of low pressure over the Asian continent and higher pressure over the Arabian Sea. Persistent northwesterly winds (2–13 $m\ s^{-1}$) over the Arabian Peninsula, which are driven by a pressure gradient between the Iranian highlands and the Arabian lowlands, also have the potential to deliver terrestrial material to the Arabian Sea during boreal summer (Ackerman and Cox, 1989). During boreal winter, northeasterly winds (2–4 $m\ s^{-1}$) associated with the Indian winter monsoon blow from Asia toward the Arabian Sea, thereby introducing material from southern Asia to the Arabian Sea (Ramage et al., 1972).

In order to reconstruct the intensity of the Indian monsoon through time, it is critical to have a means of determining the strength of the winds described above. Past wind strength can be inferred directly via the concentration of eolian material, such as dust (*e.g.* Sirocko et al., 2000), or indirectly via proxies for wind–induced upwelling (*e.g.* Overpeck et al., 1996; Anderson et al., 2002) in marine sediments. Eolian–derived plant waxes have the potential to be direct proxies for

both wind strength and trajectory (*e.g.* Ohkouchi et al., 1997; Huang et al., 2000; Rommerskirchen et al., 2003; Schefuß et al., 2003). Sedimentary plant wax records may also reflect changes in the source area of the compounds through time. Changes in plant wax source area through time must be constrained prior to inferring changes in wind strength.

1.1 Terrestrial Plant Waxes

Terrestrial plant leaf waxes, produced by all higher plants (Gulz, 1994), contain long–chain ($C_{25}-C_{36}$) *n*–alkanes, *n*–alcohols, and *n*–alkanoic acids that serve as protection against dessication and bacterial attack (Eglinton and Hamilton, 1963; Cox et al., 1982; Simoneit et al., 1977; Brassell, 1993; Collister et al., 1994; Simoneit, 1997). These compounds are periodically ablated from living plants by wind (Hadley and Smith, 1989) and can therefore be analyzed in sediments as a means of reconstructing eolian input to the marine environment (*e.g.* Ohkouchi et al., 1997; Huang et al., 2000; Rommerskirchen et al., 2003). Plant waxes in marine sediments on coastal margins can also be fluvially derived (*e.g.* Prahl et al., 1994; Kienast et al., 2003; Pelejero, 2003; Hughen et al., 2004). It is also important to note that ancient plant waxes in soils and dessicated lakes may be delivered to the marine environment by winds or rivers (*e.g.* Eglinton et al., 1997, 2002).

In principle, any one of the three primary lipids groups comprising plant waxes can be used to characterize terrestrial plant wax inputs to marine sediments. As noted by Simoneit (1997) and Huang et al. (2000) in their studies of all three of these classes of lipids, the carbon isotopic composition of the *n*–alkanoic acids correlated nearly 1:1 with the carbon isotopic composition of the *n*–alkanes. This good correlation confirms what was predicted from biosynthetic considerations by Gulz (1994) as well as from observations (*e.g.* Collister et al., 1994; Conte and Weber, 2002; Chikaraishi et al., 2004) and reflects the fact that *n*–alkanes are biosynthesized from *n*–alkanoic acids (Cheesbrough and Kolattukudy, 1984; Post-Beittenmiler, 1996).

In terms of their abundance in marine sediments, *n*–alkanoic acids are generally as abundant as *n*–alkanes (*e.g.* Huang et al., 2000), if not more abundant (K. Hughen, unpublished data). We have chosen to study the *n*–alkanoic acids because of their abundance in sediments and because they are not subject to contamination by fossil hydrocarbons, as *n*–alkanes commonly are (Eglinton et al., 1997; Pearson and Eglinton, 2000). Given that the Arabian Sea region is very close to regions with high abundances of petroleum, this study concentrates on *n*–alkanoic acids rather than on *n*–alkanes.

1.2 Sedimentation in the Arabian Sea

Lithogenic material is delivered to the Arabian Sea via many sources, both fluvial and eolian (Sirocko and Lange, 1991, and references therein). The primary fluvial sources of sediment are the Indus River, the Tapti and Narmada Rivers, and runoff from the Makran Margin. The primary regions providing a source of eolian material are the Arabian Peninsula, Eastern Africa, and Pakistan/Northern India. Because terrestrial plant waxes can be delivered to sediments by both winds and rivers, it is important to consider the modern potential eolian and fluvial inputs of sediment to our core locations.

The Indus Fan is the second largest deep–sea fan in the world, reflecting the high discharge of sediments from the Himalayas, which are drained by the Indus River (Kolla and Coumes, 1987; Prins et al., 2000a). A study by Prins et al. (2000a, closed square on Figure 2) has shown that during glacial low–stands during the Quaternary period, material from the Indus River was deposited on the middle fan. Between 8,000 and 10,000 years ago, however, when sea level had risen to near present–day levels, eolian dusts from the Arabian Peninsula began to dominate terrigenous sedimentation on the middle fan (Prins et al., 2000a). Indus sediments are presently deposited on the inner shelf and in the Ranns of Kutch, a subaerially exposed region within the southeast

corner of the Indus Delta (Wells and Coleman, 1984; von Rad and Tahir, 1997). The outer shelf is currently characterized by a lack of deposition (von Rad and Tahir, 1997). The Murray Ridge, located to the east of site 57KL on Figure 2, prevents Indus material from being deposited in the Gulf of Oman (Wells and Coleman, 1984).

Deposition and redistribution of fluvial material is more significant on the Makran Margin than on the Indus Margin (Staubwasser and Sirocko, 2001). While sediment input from the many small rivers that drain this region was higher during glacial times than it is today, there is still active fluvial sedimentation on the Makran Margin (von Rad et al., 1999; Prins et al., 2000b). A study of the clay mineralogy of the same core–top sediments used in this study revealed that the accumulation rate of chlorite, the source of which is the Makran Margin, has a maximum in the Gulf of Oman that diminishes southeastward (Sirocko et al., 1991). Site 57KL, used in both this study and in Sirocko et al. (1991), is on the tail end of that maximum and is thus likely to have a significant fluvial influence from the Makran region (Figure 2).

A number of small rivers draining from the Indian subcontinent into the eastern Arabian Sea also deliver fine–grained material to sediments. The largest of these rivers are the Tapti and Narmada. Deposition from these rivers occurs mainly on the continental shelf and is linked to topographic depressions on the seafloor (Sirocko et al., 1991, and references therein).

Despite the number of rivers draining into the Arabian Sea, eolian fluxes dominate lithogenic sedimentation in areas of hemipelagic, non–turbidite deposition (Sirocko and Sarnthein, 1989). The main source of dust to the Arabian Sea is the Arabian Peninsula/Mesopotamia region (Tindale and Pease, 1999, and references therein). The two other primary dust sources are Eastern Africa and the Asian continent (*e.g.* Sirocko et al., 2000).

1.3 Compound Specific Isotope Analysis

The carbon isotopic composition of leaf waxes is determined by several factors, including the local abundance and isotopic composition of atmospheric carbon dioxide, temperature, and aridity (Cerling et al., 1997; Street-Perrott et al., 1997; Kuypers et al., 1999; Pagani et al., 1999). These three factors are reflected in the photosynthetic pathway utilized by the plant. The two main pathways, C_3 and C_4, differ in the extent to which they discriminate against ^{13}C relative to ^{12}C. C_3 plants, found in forests and high–latitude grasslands, have carbon isotopic compositions ranging from $-25‰$ to $-30‰$ (Collister et al., 1994). The C_4 pathway is used primarily by plants in arid and semiarid environments, such as tropical grasslands. C_4 plants have a $\delta^{13}C$ of $-10‰$ to $-16‰$ (Collister et al., 1994). Lipids are depleted in ^{13}C relative to bulk plant tissue by $4 - 8‰$ (Rieley et al., 1991, 1993; Collister et al., 1994; Chikaraishi et al., 2004). The compounds utilized for this study, *n*–alkanoic acids, exhibit isotopic compositions of $-38‰$ for C_3 plants and $-20‰$ for C_4 plants (Chikaraishi et al., 2004). Because the carbon isotopic compostions of C_3 and C_4 plants are offset from one another, the $\delta^{13}C$ of terrestrial plant waxes in marine sediments can be interpreted using a two end–member mixing model reflecting the relative inputs of C_3 and C_4 plants. It is important to note that the isotopic composition of long–chain fatty acids is not significantly affected by early diagenesis (Haraoka and Ishiwarati, 2000).

Sixty–six percent of the total land area in the Middle Eastern and African regions that surround the Arabian Sea has sparse or barren vegetation (Food and Agriculture Organization of the United Nations (FAO), 2002; Development Data Group, The World Bank, 2002). Shrublands, savanna, and grasslands compose 25% of the remaining land area and are the most prevalent types of vegetated land cover in these regions (Food and Agriculture Organization of the United Nations (FAO), 2002; Development Data Group, The World Bank, 2002). These vegetation types are characterized by C_4 plants (Cerling et al., 1993). The natural vegetation of India and Pakistan, the primary coun-

tries from which Asian plant waxes would be derived, is also largely shrubland and grassland (Food and Agriculture Organization of the United Nations (FAO), 2002; Development Data Group, The World Bank, 2002). The Mesopotamian region, located between the Tigris and Euphrates Rivers in modern day Iraq, contains over 20,000 km^2 of marshlands within which reed beds of *Typha* and *Phragmites* are the main vegetation types. Both *Typha* and *Phragmites* are C_3 terrestrial emergent vascular plants (Sermolli, 1957; Cloern et al., 2002).

We hypothesized that the modern core–top accumulation rates and isotopic compositions of plant waxes in the Arabian Sea would reflect the three main potential sources of fluvial and eolian material to the Arabian Sea: Africa, the Arabian Peninsula/Mesopotamian region, and Asia. Given the abundance of C_4 vegetation throughout the Arabian Sea region, we expected that the $\delta^{13}C$ of plant waxes would reflect largely C_4 sources.

2 MATERIALS AND METHODS

2.1 Surface Sediments

Many of the surface sediments used in this study (Figure 2) came from the core–top sample set of Sirocko and Sarnthein (1989). As many of these original samples have been depleted, we have supplemented this sample set with a number of multicores from the western Arabian Sea. Two box cores were obtained during the R/V Sonne-28 cruise in 1983. Seven 5 m long box cores were obtained during the R/V Sonne-42 cruise. Two piston cores were obtained during leg IOE. One core was obtained on Meteor–5. Core tops of seven multicores, recovered as part of the JGOFS program during cruises TN–41 and TN–47, were also analyzed. Table 1 shows a complete list of samples used in this study.

2.2 Analytical Methods

Multicore samples were freeze–dried overnight. All other samples were oven dried at 60°C. Samples were crushed gently prior to the extraction of the lipid biomarkers. A total lipid extract (TLE) was isolated using Accelerated Solvent Extraction (ASE; 1000psi, 100°C, 9:1 dichloromethane: methanol). The TLE was then evaporated to a small volume and applied to an aminopropyl column (Supelco LC–NH_2, 0.5 g). The non–polar fraction was eluted with 7 mL of 9:1 dichloromethane:acetone. The polar fraction, containing the *n*–alkanoic acids, was eluted with 8 mL of 2% formic acid in dichloromethane. This latter fraction was taken to dryness and transesterified overnight at 70°C using 95:5 methanol:HCl. The methanol had a known isotopic composition of $-47.25‰$. The resultant fatty acid methyl esters (FAMES) were partitioned into the organic phase by adding 20 mL of milli–Q water and 10 mL of hexane to each vial. After sonicating for 5 minutes to ensure that the liquid/liquid extraction was complete, the hexane fraction was applied to a sodium sulfate column to remove residual water. The liquid/liquid extraction was then repeated twice with 5 mL aliquots of hexane that were also applied to the sodium sulfate column. Samples were then taken to dryness. An aliquot of the sample was dried down, redissolved in 50:50 pyridine:bis(trimethylsilyl)trifluoroacetamide (BSTFA), and heated at 70°C for 15 minutes prior to analysis by gas chromatography–mass spectrometry (GC–MS).

GC–MS analyses were performed using an HP 6890 gas chromatograph fitted with a J&W DB–5 column and coupled to an HP 5973 mass–selective detector. The GC–MS temperature program was: 40°C (isothermal) for 1 minute, 20°C/minute to 120°C, hold for 5 minutes, 10°C/minute to 320°C, hold for 20 minutes. C_{22}–C_{32} FAMES eluted between 25 and 40 minutes. Compound specific carbon isotope analyses were performed on the FAMES via gas chromatography–isotope ratio mass spectrometry (GC–irMS) using a Finnigan Delta^{Plus} isotope mass spectrometer coupled to an HP 6890 gas chromatograph. The temperature program for the GC–irMS was similar to that

used for GC–MS. All isotope samples were run in triplicate.

2.3 Data Analysis

FAME concentrations were determined by integrating the chromatograms generated by the flame ionization detector (FID) of the GC–MS and comparing with a standard mixture of FAMES of known concentration. We consider the total plant wax concentration to be the sum of the even–numbered homologues from $C_{24} - C_{32}$. Isotopic compositions were determined for each individual homologue by averaging the values obtained in the three replicate analyses. Carbon isotopic values were calibrated to several CO_2 pulses of known isotopic composition. Instrument error, determined via repeated measurements of a suite of nine standards, is estimated to be $0.3‰$. The average standard deviation ($\pm 1\sigma$) for triplicate analyses of the C_{30} alkanoic acid was $0.44‰$. For cases in which the isotopic composition of one member of the triplicate was greater than $1‰$ different from the other two members, the average of the other two values was used. By this method, members of the triplicate that were significantly different at the greater than 2σ level from the other two analyses were excluded. The isotopic composition of each homologue was then corrected for the addition of the methyl group during transesterification using a mass–balance approach.

Plant wax accumulation rates were calculated using the age models, sedimentation rates, and dry bulk densities given in Sirocko et al. (2000) for all Sonne, IOE, and Meteor cores. Sedimentation rates for all TN multicores are based on a minimum of two radiocarbon dates per multicore, with the exceptions of 17MC, for which the sedimentation rate was calculated using core TN47-01MC, located at the same site but taken during a later cruise, and 12MC, for which the sedimentation rate was estimated to be between the sedimentation rates of 16MC and 17MC. All multicore radiocarbon dates were determined at the National Ocean Sciences Accelerator Mass Spectrometry (NOSAMS) Facility in Woods Hole (Table 2). Dry bulk densities of TN samples were determined

by oven drying a known volume (typically $\sim$5 cc) of sediment and weighing.

3 RESULTS AND DISCUSSION

3.1 Accumulation Rates

Total terrestrial plant wax fatty acid concentrations ranged from 0.054–11.4 μg/gdw, corresponding to accumulation rates of 0.048–59.3 μg cm^{-2} kyr^{-1} (Figure 3). The range in concentrations exhibited in the Arabian Sea is consistent with Holocene concentrations observed in a variety of other settings including eolian–dominated sites such as the West African Margin (0.5–0.8 μg cm^2 kyr^{-1} for *n*–alkanoic acids; Huang et al., 2000), the Central Pacific (0.1–1.5 μg cm^2 kyr^{-1} for *n*–alkanes; Ohkouchi et al., 1997), and the South China Sea (0–1.5 μg cm^2 kyr^{-1} for the C_{29}–alkane; Pelejero, 2003), as well as fluvially–dominated sites such as the Cariaco Basin (3–30 μg cm^2 kyr^{-1} for *n*–alkanoic acids; Hughen et al., 2004). The spatial patterns described in this section for the total plant wax fraction also hold true for the concentrations and accumulation rates of individual homologues.

The highest plant wax accumulation rates occur within the Gulf of Oman (Site 422; 59.3 μg cm^{-2} kyr^{-1}) and along the Somali Margin (Site 143KK; 51.8 μg cm^{-2} kyr^{-1}), two sites where the lithogenic sedimentation is primarily fluvial (Sirocko et al., 1991). Consistent with the extent of Makran Margin–derived chlorite, accumulation rates are also very high at site 57KL, in the northwest Arabian Sea (Sirocko et al., 1991). Because these three sites are clearly affected by fluvial sedimentation, they are unlikely to be useful locations for eolian reconstructions. Given the current state of knowledge regarding present–day sedimentation in the Arabian Sea, however, plant waxes at the remaining sites are likely delivered by winds (Wells and Coleman, 1984; Sirocko and Sarnthein, 1989; von Rad and Tahir, 1997; Prins et al., 2000a).

Excluding the three sites just described, several general trends in plant wax accumulation rates can be observed in Figure 3. Accumulation rates decrease from the Somali Margin (site 114KK) toward the interior of the Arabian Sea, likely reflecting a source of plant waxes derived from Africa. A northwest–southeast gradient extends offshore of the Oman Margin, reflecting a source of plant waxes derived from the summertime northwesterly winds that blow over the Arabian Peninsula. A third, and weaker, gradient can be observed from the Indian subcontinent (sites 26KL and 36KL) to the interior of the Arabian Sea (*e.g.* site 15KL). As is evident in Figure 3, not all sites are consistent with these gradients. This is likely the result of the errors associated with estimation of sedimentation rates. In summary, the accumulation rate data suggest three eolian sources of plant waxes to the Arabian Sea: Africa, Asia, and the Arabian Peninsula/Mesopotamian region (hereafter APM).

The gradients observed in plant wax accumulation rates are similar to those of other studies investigating modern day eolian dust inputs to the Arabian Sea (*e.g.* Tindale and Pease, 1999; Sirocko et al., 2000). Satellite, sediment trap, and surface sediment data have demonstrated that the northeast monsoon does not transport significant quantities of dust to the Arabian Sea (Sirocko and Sarnthein, 1989; Clemens, 1998; Schulz et al., 2002). However, plant wax accumulation rates at sites affected by northeast monsoon winds are lower than at sites affected by the southwest monsoon winds and roughly equal to those at sites affected by the northwesterly winds. This suggests that the winds of the northeast monsoon do provide a source of plant waxes to the Arabian Sea.

Despite their strength, the summer southwest monsoon winds are not the primary carriers of dust to the interior of the Arabian Sea because the Findlater Jet forms in the relatively dust free equatorial region near the African margin (Tindale and Pease, 1999). Nevertheless, African dust, with a characteristically high Zr/Hf ratio, has been identified in core–top sediments, which sug-

gests that dust deposition during the southwest monsoon is significant (Sirocko et al., 2000). Furthermore, East African pollen types have been observed downwind of Somalia during the summer southwest monsoon (Van Campo, 1991). We find relatively high accumulation rates of plant waxes at site 114KK, along the Somali Margin, suggesting that southwest monsoon winds transport leaf waxes, as well as pollen and dust, from Eastern Africa to the Arabian Sea.

The main source of mineral dust to the Arabian Sea is the Arabian Peninsula, over which northwesterly winds blow during the summer (Sirocko and Sarnthein, 1989; Sirocko et al., 1991; Tindale and Pease, 1999, and references therein). The aridity and availability of desert dust in the APM region allows for efficient advection of fine material, even though the northwesterly winds are less intense than the winds of both the southwest and northeast monsoons. The Arabian Peninsula is also a source of pollen to the Arabian Sea (Van Campo, 1991). Similar to the results for dust inputs, we find that the northwesterly winds deliver a significant amount plant waxes to the Arabian Sea. As plant waxes are commonly associated with eolian dust (Simoneit et al., 1977; Cox et al., 1982; Peltzer and Gagosian, 1987; Poynter et al., 1989; Huang et al., 2000; Schefuß et al., 2003), this is to be expected.

3.2 Carbon Isotopes

Compound–specific δ^{13}C of the plant waxes (Figure 4a) supports the notion that the compounds found in the Arabian Sea are derived from three sources. δ^{13}C values for the C_{30} alkanoic acid (hereafter $\delta^{13}C_{30}$) range from $-21‰$ to $-27‰$, reflecting contributions from both C_3 and C_4 plants throughout the region (Rieley et al., 1991, 1993; Collister et al., 1994; Chikaraishi et al., 2004). Other homologues, as well as the average values for all even–numbered homologues from C_{24}–C_{32}, show similar trends and isotopic compositions.

In order to quantify the relative contributions of C_3 and C_4 plant waxes to the total observed

carbon isotopic composition for the C_{30} alkanoic acid at different sites, we have defined a two end–member model with the δ^{13}C of C_3 and C_4 *n*–alkanoic acids as $-38‰$ and $-20‰$, respectively (Chikaraishi et al., 2004). These isotopic compositions are intended to be representative rather than absolute, as *n*–alkanoic acids from both C_3 and C_4 plants exhibit a range of isotopic compositions (*e.g.* Chikaraishi et al., 2004). Along the Indian and African margins, $\delta^{13}C_{30}$ values of $-21‰$ to $-23.6‰$ indicate C_4 contributions of over 80%, which reflects the abundance of exposed C_4 biomass in these regions. Along the Oman Margin, the $\delta^{13}C_{30}$ exhibits much lighter values of $-25.1‰$ to $-27‰$. These values reflect C_4 contributions of 60–75% (Figure 4b). This is somewhat surprising given the dryness of the Arabian Peninsula. However, the origin of the northwesterly winds is such that they could ablate material from the Mesopotamian region (Sirocko et al., 1991). The climate of this region is semiarid, with wet winters and hot, dry summers. Such seasonality is conducive to dust production and transport (Pye, 1989). The southern Mesopotamian plains encompass numerous shallow (<3 m) freshwater and brackish lakes as well as extensive marshes (Aqrawi, 2001) that contain C_3 plant material (*e.g. Typhus* and *Phragmites*) that could be transported to the Arabian Sea via the summertime northwesterly winds. The extent of the C_3–like $\delta^{13}C_{30}$ values is similar to the extent of high dolomite accumulation rates (Figure 5) observed by Sirocko et al. (1991). Mesopotamian dusts are known to be rich in dolomite. Both dolomite and plant waxes may therefore be derived from the Mesopotamian region. Thus, despite the weakness of the northwesterlies relative to the southwest and northeast monsoon winds, these winds are an important source of C_3 plant waxes to the Arabian Sea.

3.3 Homologue distributions

The Carbon Preference Index (CPI; the sum of the even carbon–numbered *n*–alkanoic acids from C_{24} to C_{32} divided by the sum odd carbon–numbered *n*–alkanoic acids from C_{23} to C_{31}) of the

Arabian Sea samples ranges from 3.1–6.6. The CPI is a measure of the degree of degradation of the *n*–alkanoic acids, which, when unaltered, have a strong even–over–odd predominance (Brassell, 1993). There do not appear to be any geographic trends in the CPI in the Arabian Sea (not shown), which suggests that the accumulation rate and carbon isotopic trends evidenced throughout the Arabian Sea are not significantly affected by diagenetic overprinting. CPI values calculated in this study compare well to those observed along the west African margin by Huang et al. (2000) and Rommerskirchen et al. (2003).

We also find no evidence for a correlation between the Average Chain Length (ACL; $\Sigma(C_i{*}i)/\Sigma C_i$, where C_i is the concentration of an *n*–alkanoic acid of chain–length *i*) of *n*–alkanoic acids and their carbon isotopic composition in the Arabian Sea. Such a relationship has been noted in several studies from the west African margin and the Cariaco basin (Rommerskirchen et al., 2003; Schefuß et al., 2003; Hughen et al., 2004) using a variety of different means of calculating ACL. In contrast, ACL values from the Arabian Sea, calculated for all homologues C_{24}–C_{32} as well as subsets including only the highest abundance homologues, show no correlation to $\delta^{13}C$.

3.4 Plant wax ages

While the plant waxes analyzed in this study do come from core–top sediments, two concerns arise regarding the age of the waxes. First, it must be established that the surface sediments containing the waxes are, in fact, modern. Radiocarbon ages confirm that the surface sediments of all of the TN multicores are less than 4000 years old. When a standard 400 year reservoir correction is applied, two of these cores (11MC and 16MC) have ages of about 50 years. Similarly, the surface sample from core 74KL has an age between 1230 and 3350 years. The surface ages of the rest of the cores used in this study have not been determined via ^{14}C dating. However, applying the sedimentation rates reported by Sirocko et al. (1991) to the depth ranges given in Table 1 for

each core shows that the age range represented by each sample is less than 2 kyr in all but two cases (11KL: 2.35 kyr and 18KL: 4 kyr). These sediments therefore encompass a relatively short time span. Coupled with evidence from low resolution oxygen isotope records, it is unlikely that the samples used for this study contain sediments older than a few thousand years (Sirocko, 1989, 1995).

The second concern is whether the plant waxes found in modern sediments are, in fact, modern themselves, or whether they are "pre–aged." While it is generally assumed that the different components of a given sediment horizon are contemporaneous, this is not always the case. For example, plant waxes contained within eolian dust collected off Northwest Africa exhibit ^{14}C ages of $\sim$650 years, likely the result of a mixture of waxes derived from modern vegetation and from dessicated lake sediments and/or soils (Eglinton et al., 2002). Given that the climate of the Middle East was generally wetter prior to $\sim$4 kyr B.P. than it is today (*e.g.* Cullen et al., 2000; Aqrawi, 2001, and references therein), there are potential sources of C_3 plant waxes from dessicated lake beds throughout the Arabian Sea region. In this case, it would be possible for the C_3–like δ^{13}C signature seen in core–top sediments off the coast of Oman to be derived from pre–aged plant waxes from the Arabian Peninsula rather than being derived from the modern C_3 sources within Mesopotamia. While this possiblity does exist, it is unlikely for the following reason. Dessicated lake beds containing C_3 plant material should be present throughout the Arabian Sea region, not just on the Arabian Peninsula, as both East Africa (*e.g.* Gasse, 2000, and references therein) and southern Asia (*e.g.* Enzel et al., 1999) also experienced a drying during the mid–Holocene. Thus, the three major wind systems in the region could all be delivering pre–aged waxes to the Arabian Sea. If this were the case, then there would be no clear C_3 signal off of the Arabian Peninsula. The fact that this signal is so clear indicates either that lake beds containing C_3 plant material are found only on the Arabian Peninsula (unlikely given the generalized mid–Holocene aridification of the

region) or that any pre–aged plant wax material from Asia and Africa is swamped by a modern, C_4 signature while the signal from Mesopotamia plus the Arabian Peninsula is not. While this second option cannot be ruled out, it seems unlikely given that all three major source regions are deserts and should therefore have similar potentials for eolian deflation. These concerns could be further addressed by compound–specific ^{14}C dating of the plant waxes in core–top sediments throughout the Arabian Sea.

3.5 Controls on the deposition of plant waxes in the Arabian Sea

While the transportation of plant waxes from the APM region is dependent upon the northwesterlies, the deposition of these waxes in the Arabian Sea is likely dependent upon the strength of the southwest monsoon. Eolian material is subject to both dry and wet deposition. In the absence of rainfall, fine particles can be carried over great distances (*e.g.* Ohkouchi et al., 1997, and references therein). In this case, the removal is dependent upon both wind strength and particle density. However, particulate material can also be removed from the air via precipitation (Duce, 1995). During the summer, when both the northwesterlies and the southwesterlies are active, the hot, dry northwesterlies overlie the moist southwesterlies (Findlater, 1969, and references therein). The height of the boundary between the two air masses, known as the monsoon inversion, increases from west to east and depends upon the strength of the southwest winds (Narayanan and Rao, 1981). When the southwest monsoon is strong, the inversion is confined to the region west of 65°E (Narayanan and Rao, 1981). The transportation of dust and other eolian material is therefore blocked from the interior of the Arabian Sea. However, when the southwest winds are weak, such as during a break period, the inversion moves eastward toward the Indian subcontinent and material contained within the northwesterly winds can be transported further out into the Arabian Sea (Figure 6). Transportation of eolian material to the interior of the Arabian Sea is therefore strongly

dependent upon the moist southwesterly winds of the summer monsoon (Tindale and Pease, 1999). Accordingly, the spatial extent of ^{13}C–depleted plant wax fatty acids (Figure 4a) and high dolomite accumulation rates (Figure 5) correlate well with the approximate position of the monsoon inversion during an active phase, as determined by Narayanan and Rao (1981, Figure 6). This suggests that the west–to–east δ^{13}C gradient in the Arabian Sea can potentially be used as an indicator of the position of the monsoon inversion, and therefore of the relationship between the southwesterly and northwesterly winds, and, by extension, the intensity of the southwest monsoon. One potential complication in the interpretation of temporal changes in plant wax accumulation rate is the uncertainty of the magnitude of fluvial inputs through time. In the Arabian Sea, lowered sea level during the Last Glacial Maximum allowed for the sedimentation of Indus–derived material as far from the continent as the middle fan, where lithogenic sedimentation today is eolian (Prins et al., 2000a).

Based on the above findings, downcore reconstructions of the southwest monsoon in this manner would benefit from using a combination of both dolomite accumulation rates and plant wax δ^{13}C. Alone, variations in dolomite accumulation rates could reflect changes in Mesopotamian aridity, northwesterly wind strength, and southwesterly wind strength. Within the source region, plant wax δ^{13}C, unlike dolomite, responds to aridity. Thus plant wax δ^{13}C potentially can be used to infer changes in Mesopotamian aridity as well as changes in the relationship between the northwesterly and southwesterly winds. For example, if plant wax δ^{13}C along the Oman margin became less depleted and dolomite accumulation rates decreased, the cause would likely be an increase in summer monsoon wind strength. However, if plant wax δ^{13}C became less depleted and dolomite accumulation rates increased, the cause would likely be increased Mesopotamian aridity. Such an approach would ideally be complimented by the utilization of a biomarker for fluvial input, such as lignin (Goñi et al., 1998), in order to constrain changes in riverine input through time.

4 CONCLUSIONS

Based on the accumulation rate and δ^{13}C compositions of terrestrial plant wax *n*–alkanoic acids, we have determined that leaf waxes are delivered to the Arabian Sea from sources in Asia, Africa, and the Arabian Peninsula/Mesopotamian region. The carbon isotopic composition of vascular plant fatty acids in modern sediments reflects the vegetation of the land masses surrounding the Arabian Sea. Plant waxes derived from Asia and Africa reflect C_4 contributions of $\sim$80% while plant waxes derived from the Arabian Sea/Mesopotamian region reflect a greater influence (25% or more) of C_3 plants. These data are consistent with modern–day observations of dust and pollen inputs to the Arabian Sea (Van Campo, 1991; Tindale and Pease, 1999), as well as with surface sediment dust data (Sirocko et al., 2000). The extent of the modern transport of plant waxes (as indicated by the geographic extent of plant waxes with C_3 contributions of over 25%) correlates well with the modern–day boundary between the dry northwesterly and moist southwesterly winds that develop during the summer. The transport of eolian material to the interior of the Arabian Sea via the northwesterly winds is limited by the presence of the moist southwesterly winds associated with the Indian summer monsoon. These winds effectively create a barrier that prevents dust and plant waxes carried by northwesterly winds from reaching into the central Arabian Sea. We therefore hypothesize that the west–to–east gradient in plant wax δ^{13}C across the Arabian Sea could provide a means for reconstructing the relationship between the summer northwesterly and southwesterly winds and, therefore, the strength of the southwest monsoon itself. This approach would be even more powerful when used in conjunction with dolomite accumulation rates, as both Mesopotamian aridity and southwest monsoon strength could be deduced.

Acknowledgments

We thank Sean Sylva and Carl Johnson for technical assistance. We also thank Dorinda Ostermann and Luping Zou for their assitance in the preparation of samples for radiocarbon work. The comments of three anonymous reviewers significantly improved this manuscript. This work was supported by a SGER grant from the National Science Foundation to D.O. and a Schlanger Ocean Drilling Fellowship to K.D.

References

Ackerman, S. A., Cox, S. K., 1989. Surface weather observations of atmospheric dust over the southwest summer monsoon region. Meteorol. Atmos. Phys. 41, 19–34.

Anderson, D. M., Overpeck, J. T., Gupta, A. K., 2002. Increase in the Asian southwest monsoon during the past four centuries. Science 297, 596–599.

Aqrawi, A. A. M., 2001. Stratigraphic signatures of climatic change during the Holocene evolution of the Tigris–Euphrates delta, lower Mesopotamia. Global Planet. Change 28, 267–283.

Brassell, S. C., 1993. Applications of biomarkers for delineating marine paleoclimatic fluctuations during the Pleistocene. In: Engel, M. H., Macko, S. A. (Eds.), Organic Geochemistry. Plenum Press, New York, pp. 699–737.

Cerling, T. E., Harris, J. M., MacFadden, B. J., Leakey, M. G., Quade, J., Eisenmann, V., Ehleringer, J. R., 1997. Global vegetation change through the Miocene/Pliocene boundary. Nature 389, 153–158.

Cerling, T. E., Want, Y., Quade, J., 1993. Expansion of C_4 ecosystems as an indicator of global ecological change in the late Miocene. Nature 361, 344–345.

Cheesbrough, T. M., Kolattukudy, P. E., 1984. Alkane biosynthesis by decarbonylation of aldehydes catalyzed by a particulate preparation from *Pisum sativum*. Proceedings of the National Academy of Sciences of the United States of America 81, 6613–6617.

Chikaraishi, Y., Naraoka, H., Poulson, S. R., 2004. Hydrogen and carbon isotopic fractionations of lipid biosynthesis amount terrestrial (C3, C4, and CAM) and aquatic plants. Phytochemistry 65, 1369–1381.

Clemens, S. C., 1998. Dust response to seasonal atmospheric forcing: Proxy evaluation and calibration. Paleoceanography 13, 471–490.

Cloern, J. E., Canuel, E. A., Harris, D., 2002. Stable carbon and nitrogen isotope composition of aquatic and terrestrial plants of the San Francisco Bay estruarine system. Limnology and Oceanography 47, 713–729.

Collister, J. W., Rieley, G., Stern, B., Eglinton, G., Fry, B., 1994. Compound–specific δ^{13}C analyses of leaf lipids from plants with differing carbon dioxide metabolisms. Org. Geochem. 21, 619–627.

Conte, M. H., Weber, J. C., 2002. Plant biomarkers in aeorsols record isotpic discrimination of terrestrial photosynthesis. Nature 417, 639–641.

Cox, R. E., Mazurek, M. M., Simoneit, B. R. T., 1982. Lipids in Harmattan aerosols of Nigeria. Nature 296, 848–849.

Cullen, H. M., deMenocal, P. B., Hemming, S., Hemming, G., Brown, F. H., Guilderson, T., Sirocko, F., 2000. Climate change and the collapse of the Akkadian empire: Evidence from the deep sea. Geology 28, 379–382.

Development Data Group, The World Bank, 2002. World Development Indicators 2002 online. http://publications.worldbank.org.

Duce, R. A., 1995. Sources, distributions, and fluxes of mineral aerosols and their relationship to climate. In: Charlson, R. J., Heintzenberg, J. E. (Eds.), Aerosol Forcing of Climate. Wiley, New York, pp. 43–72.

Eglinton, G., Hamilton, R. J., 1963. The distribution of *n*–alkanes. In: Swain, T. (Ed.), Chemical Plant Taxonomy. Academic Press, pp. 187–217.

Eglinton, T. I., Benitez-Nelson, B. C., Pearson, A., McNichol, A. P., Bauer, J. E., Druffel, E. R. M., 1997. Variability in radiocarbon ages of individual organic compounds from marine sediments. Science 277, 796–799.

Eglinton, T. I., Eglinton, G., Dupont, L., Sholkovitz, E. R., Montluçon, D., Reddy, C. M., 2002. Composition, age, and provenance of organic matter in NW African dust over the Atlantic Ocean. Geochemistry, Geophysics, Geosystems 3, 10.1029/2001GC000269.

Enzel, Y., Ely, L. L., Mishra, S., Ramesh, R., Amit, R., Lazar, B., Rajaguru, S. N., Baker, V. R., Sandler, A., 1999. High–resolution Holocene environmental changes in the Thar desert, north–western India. Science 284, 125–128.

Findlater, J., 1969. A major low–level air current near the Indian Ocean during the northern summer. Quart. J. R. Met. Soc. 95, 362–380.

Food and Agriculture Organization of the United Nations (FAO), 2002. Faostat on–line statistical service. http://apps.fao.org.

Gasse, F., 2000. Hyrological changes in the African tropics since the Last Glacial Maximum. Quat. Sci. Rev. 19, 189–211.

Goñi, M. A., Ruttenberg, K. C., Eglinton, T. I., 1998. A reassessment of the sources and importance of land–derived organic matter in surface sediments from the Gulf of Mexico. Geochim. Cosmochim. Acta 62, 3055–3075.

Gulz, P.-G., 1994. Epicuticular leaf waxes in the evolution of the plant kingdom. J. Plant Physiol. 143, 453–464.

Hadley, J. L., Smith, W. K., 1989. Wind erosion of leaf surface wax in alpine timberline conifers. Arctic Alpine Res. 21, 392–398.

Haraoka, H., Ishiwarati, R., 2000. Molecular and isotopic abundances of long chain *n*–fatty acids in open marine sediments of the western North Pacific. Chemical Geology 165, 23–36.

Huang, Y., Dupont, L., Sarnthein, M., Hayes, J. M., Eglinton, G., 2000. Mapping of C_4 plant input from North West Africa into North East Atlantic sediments. Geochim. Cosmochim. Acta 64, 3505–3513.

Hughen, K. A., Eglinton, T. I., Xu, L., Makou, M., 2004. Abrupt tropical vegetation response to rapid climate changes. Science 304, 1955–1959.

Kienast, M., Hanebuth, T. J. J., Pelejero, C., Steinke, S., 2003. Synchroneity of meltwater pulse 1a and the Bølling warming: New evidence from the South China Sea. Geology 31, 67–70.

Kolla, V., Coumes, F., 1987. Morphology, internal structure, seismic stratigraphy, and sedimentation on the Indus Fan. Am. Assoc. Petrol. Geol. Bull. 71, 650–677.

Kuypers, M. M. M., Pancost, R. D., Sinninge-Damste, J. S., 1999. A large and abrupt fall in atmospheric CO_2 concentration during Cretaceous times. Nature 399, 342–345.

Narayanan, M. S., Rao, B. M., 1981. Detection of monsoon inversion by TIROS–N satellite. Nature 294, 546–548.

Ohkouchi, N., Kawamura, K., Taira, A., 1997. Molecular paleoclimatology: reconstruction of climate variabilities in the late Quaternary. Org. Geochem. 27, 173–183.

Overpeck, J. T., Anderson, D. M., Trumbore, S., Prell, W. L., 1996. The Southwest Monsoon over the last 18,000 years. Clim. Dyn. 12, 213–225.

Pagani, M., Freeman, K. H., Arthur, M. A., 1999. Late Miocene atmospheric CO_2 concentrations and the expansion of C_4 grasses. Science 285, 876–879.

Pearson, A., Eglinton, T. I., 2000. The origin of *n*–alkanes in Santa Monica Basin surface sediment: a model based on compound–specific $\Delta^{14}C$ and $\delta^{13}C$ data. Org. Geochem. 31, 1103–1116.

Pelejero, C., 2003. Terrigenous *n*–alkane input in the South China Sea: high–resolution records and surface sediments. Chemical Geology 200, 89–103.

Peltzer, E. T., Gagosian, R. B., 1987. Sampling and quantitation of lipids in aerosols from the remote marine atmosphere. Analytica Chimica Acta 198, 125–144.

Post-Beittenmiler, D., 1996. Biochemistry and molecular biology of wax production in plants. Annual Reviews of Plant Physiology and Plant Molecular Biology 47, 405–430.

Poynter, J. G., Farrimond, P., Robinson, N., Eglinton, G., 1989. Aeolian–derived higher plant lipids in the marine sedimentary record: links with palaeoclimate. In: Leinen, M., Sarnthein, M. (Eds.), Paleoclimatology and Paleometeorology: Modern and Past Patterns of Global Atmospheric Transport. Vol. 282 of NATO ASI series, Series C. Kluwer Academic Publishers, Dordrecht, pp. 435–462.

Prahl, F. G., Ertel, J. R., Goni, M. A., Sparrow, M. A., Eversmeyer, B., 1994. Terrestrial organic carbon contributions to sediments on the Washington margin. Geochim. Cosmochim. Acta 58, 3035–3048.

Prins, M. A., Postma, G., Cleveringa, J., Cramp, A., Kenyon, N. H., 2000a. Controls on terrignous sediment supply to the Arabian Sea during the late Quaternary: the Indus Fan. Marine Geology 169, 327–349.

Prins, M. A., Postma, G., Weltje, G. J., 2000b. Controls on terrignous sediment supply to the Arabian Sea during the late Quaternary: the Makran continental slope. Marine Geology 169, 351–371.

Pye, K., 1989. Processes of fine particle formation, dust source regions, and climatic changes. In: Leinin, M., Sarnthein, M. (Eds.), Paleoclimatology and Paleometeorology: Modern and Past Patterns of Global Atmospheric Transport. No. C 282 in NATO ASI Series. Kluwer, Dordrecht/Boston/London, pp. 3–30.

Ramage, C. S., Miller, F. R., Jeffries, C., 1972. Meteorological Atlas of the International Indian Ocean Expedition. The Surface Climate of 1963, 1964. US National Science Foundation and India Meteorological Department.

Rieley, G., Collister, J. W., Jones, D. M., Eglinton, G., Eakin, P. A., Fallick, A. E., 1991. Sources of sedimentary lipids deduced from stable isotope analyses of individual compounds. Nature 352, 425–427.

Rieley, G., Collister, J. W., Stern, B., Eglinton, G., 1993. Gas chromatography–isotope ratio mass spectrometry of leaf wax *n*-alkanes from plants of differing carbon dioxide metabolisms. Rapid Communications in Mass Spectrometry 7, 488–491.

Rommerskirchen, F., Eglinton, G., Dupont, L., G¨untner, U., Wenzel, C., Rullk¨otter, J., 2003. A north to south transect of Holocene southeast Atlantic continental margin sediments: Relation-

ship between aerosol transport and compound–specific δ^{13}C land plant biomarker and pollen records. Geochemistry Geophysics Geosystems 4, doi: 10.1029/2003GC000541.

Schefuß, E., Ratmeyer, V., Stuut, J.-B. W., Jansen, J. H. F., Damsté, J. S. S., 2003. Carbon isotope analyses of *n*–alkanes in dust from the lower atmosphere over the central eastern Atlantic. Geochim. Cosmochim. Acta 67, 1757–1767.

Schulz, H., vonRad, U., Ittekkot, V., 2002. Plankic foraminifera, particle flux and oceanic productivity off Pakistan, NE Arabian Sea: modern analogues and application to the paleorecord. In: Clift, P. D., Kroon, D., Gaedicke, C., Craig, J. (Eds.), The Tectonic and Climatic Evolution of the Arabian Sea Region. No. 195 in Geol. Soc. Spec. Publ. The Geological Society, London, pp. 499–516.

Sermolli, P., 1957. Una carta geobotanica dell'Africa Orientale (Eritrea, Etiopia, Somalia). Webbia XIII 1, 15–132.

Simoneit, B. R. T., 1997. Compound–specific carbon isotope analyses of individual long–chain alkanes and alkanoic acids in Harmattan aerosols. Atmos. Environ. 31, 2225–2233.

Simoneit, B. R. T., Chester, R., Eglinton, G., 1977. Biogenic lipids in particulates from the lower atmosphere over the eastern Atlantic. Nature 267, 682–685.

Sirocko, F., 1989. Zur akkumulation von Staubsedimenen im n¨ordlichen Indischen Ozean: Anzeiger der Klimagerschichte Arabiens und Indiens. Ph.D. thesis, Geologisch–Pal¨aontologisches Insitut Universit¨at Kiel.

Sirocko, F., 1995. Abrupt change in monsoonal climate: evidence from the geochemical composition of Arabian Sea sediments. Habilitation Thesis. Ph.D. thesis, University of Kiel.

Sirocko, F., Garbe-Sch¨onberg, D., Devey, C., 2000. Processes controlling trace element geochemistry of Arabian Sea sediments during the last 25,000 years. Global and Planetary Change 26, 217–303.

Sirocko, F., Lange, H., 1991. Clay–mineral accumulation rates in the Arabian Sea during the late Quaternary. Marine Geology 97, 105–119.

Sirocko, F., Sarnthein, M., 1989. Wind–borne deposits in the Northwestern Indian Ocean: Record of Holocene sediments versus satellite data. In: Leinin, M., Sarnthein, M. (Eds.), Paleoclimatology and Paleometeorology: Modern and Past Patterns of Global Atmospheric Transport. No. C 282 in NATO ASI Series. Kluwer, Dordrecht/Boston/London, pp. 401–433.

Sirocko, F., Sarnthein, M., Erlenkeuser, H., Lange, H., Arnold, M., Duplessy, J. C., 1993. Century–scale events in monsoonal climate over the past 24,000 years. Nature 364, 322–324.

Sirocko, F., Sarnthein, M., Lange, H., Erlenkeuser, H., 1991. Atmospheric summer circulation and coastal upwelling in the Arabian Sea during the Holocene and last glaciation. Quat. Res. 36, 72–93.

Staubwasser, M., Sirocko, F., 2001. On the formation of laminated sediments on the continental margin off Pakistan: the effects of sediment provenance and sediment redistribution. Marine Geology 172, 43–56.

Street-Perrott, F. A., Huang, Y., Perrott, R. A., Eglinton, G., Barker, P., Khelifa, L. B., Harkness, D. D., Olago, D. O., 1997. Impact of lower atmospheric carbon dioxide on tropical mountain ecosystems. Science 278, 1422–1426.

Tindale, N. W., Pease, P. P., 1999. Aerosols over the Arabian Sea: Atmospheric transport pathways and concentrations of dust and sea salt. Deep–Sea Research II 46, 1577–1595.

Van Campo, E., 1991. Pollen transport into Arabian Sea sediments. In: Prell, W. L., Niitsuma, N., et al. (Eds.), Proceedings of the Ocean Drilling Program, Scientific Results. Vol. 117. Ocean Drilling Program, College Station, pp. 277–280.

von Rad, U., Schulz, H., Riech, V., den Dulk, M., Berner, U., Sirocko, F., 1999. Multiple monsoon-controlled breakdown of oxygen-minimum conditions during the past 30,000 yeasr documented in laminated sediments off Pakistan. Palaeogeogr. Palaeoclim. Palaeoecol. 152, 129–161.

von Rad, U., Tahir, M., 1997. Late Quaternary sedimentation on the outer Indus shelf and slope (Pakistan): evidence from high–resolution seismic data and coring. Marine Geology 138, 193–236.

Wells, J. T., Coleman, J. M., 1984. Deltaic morphology and sedimentology, with special references to the Indus River Delta. In: Haq, B. U., Milliman, J. D. (Eds.), Marine Geology and Oceanography of Arabian Sea and Coastal Pakistan. Van Nostrand Reinhold Company Inc., New York, pp. 85–100.

Table 1. Locations of surface sediments used in this study

Cruise	Core	Core Type	Latitude	Longitude	Water Depth (m)	Sample depth (cmbsf)[a]
SO28	11KL	box	5°23.4'N	60°15.1'E	3859	0–5
SO28	18KL	box	1°54.0'N	67°20.5'E	3035	0–10
SO42	15KL	box	14°52.8'N	64°44.8'E	3920	0–5
SO42	26KL	box	15°30.9'N	68°45.6'E	3776	0–5
SO42	36KL	box	17°04.5'N	69°02.7'E	2055	0–5
SO42	51KL	box	20°57.9'N	65°33.5'E	2644	0–5
SO42	57KL	box	20°54.5'N	63°07.3'E	3422	0–5
SO42	74KL	box	14°19.3'N	57°20.8'E	3212	9–15
SO42	87KL	box	10°30.1'N	57°44.2'E	3773	0–5
IOE	114KK	piston	08°00.5'N	51°12.8'E	3843	3–8
IOE	143KK	piston	01°15.0'N	44°47.0'E	1522	12–19
Meteor5	422		24°23.4'N	59°02.5'E	2732	0–10
TN41	11MC	multi	17°26.1'N	58°47.7'E	3618	0–1
TN41	12MC	multi	16°24.1'N	60°14.2'E	4040	0–1
TN41	16MC	multi	17°13.0'N	59°36.5'E	3478	0–1
TN41	17MC	multi	15°59.7'N	61°32.0'E	3985	0–1
TN41	22MC	multi	10°02.1'N	65°05.1'E	4426	0–1
TN41	37MC	multi	19°16.1'N	58°21.1'E	784	1–1.5
TN47	20MC	multi	19°14.1'N	58°22.2'E	806	0–1

(a) centimeters below sea fbor

Table 2. Radiocarbon dates on cores used in this study

Core	Depth (cm)	Species	^{14}C age	Error	NOSAMS Acc.#
TN41-11MC	1–2	mixed planktonics	490	35	39676
TN41-11MC	47–48	G. sacculifer[a] and G. ruber (white)	1620	30	39677
TN41-16MC	0–2	G. menardii	475	25	14411
TN41-16MC	3–4	G. menardii	695	40	14412
TN41-16MC	7–8	G. menardii	710	50	15782
TN41-16MC	13–15	G. menardii	1650	25	14414
TN41-16MC	19–20	G. menardii	2130	30	14415
TN47-01MC[b]	0–1	G. menardii	1490	35	14416
TN47-01MC	3–4	G. menardii	1170	50	14417
TN47-01MC	7–8	G. menardii	3060	100	14418
TN47-01MC	13–14	G. menardii	5160	45	14419
TN41-22MC	0–1	G. menardii	3720	55	14420
TN41-22MC	7–8	G. menardii	10,750	60	14422
TN41-22MC	13–14	G. sacculifer	12,000	55	14423
TN41-22MC	19–20	G. menardii	13,100	55	16683
TN41-37MC	0–0.5	G. sacculifer	3080	55	38213
TN41-37MC	43–44	G. sacculifer	10,250	60	38214
SO42-74KL[c]	7.5	G. ruber	1230	60	
SO42-74KL[c]	35	G. ruber	3350	100	

(a) Only sacculifers without sac–like final chambers were used. (b) This site is at the same location as TN41-17MC, the multicore used in this study. Sedimentation rates for core 01MC were used to calculate accumulation rates for 17MC. (c) Uncalibrated ages as reported by Sirocko et al. (1993).

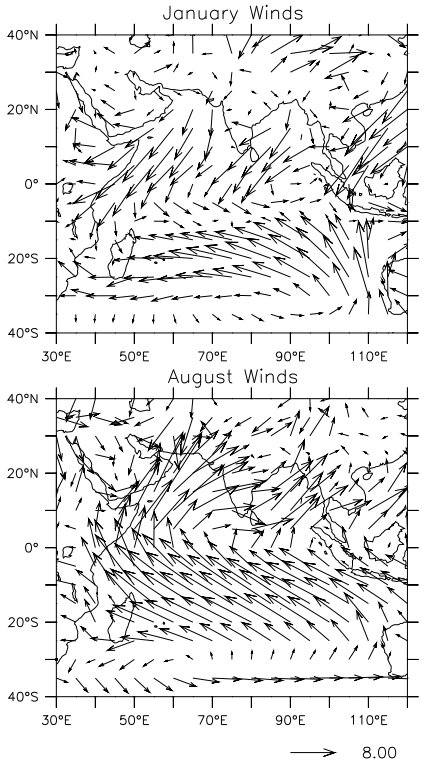

Figure 1: Winds associated with the Indian Monsoon during January (top) and August (bottom). Data are long–term monthly averages from 1968–1996. NCEP Reanalysis Data provided by the NOAA–CIRES Climate Diagnostic Center, Boulder, Colorado, from their website (http://www.cdc.noaa.gov). Units are ms^{-1}

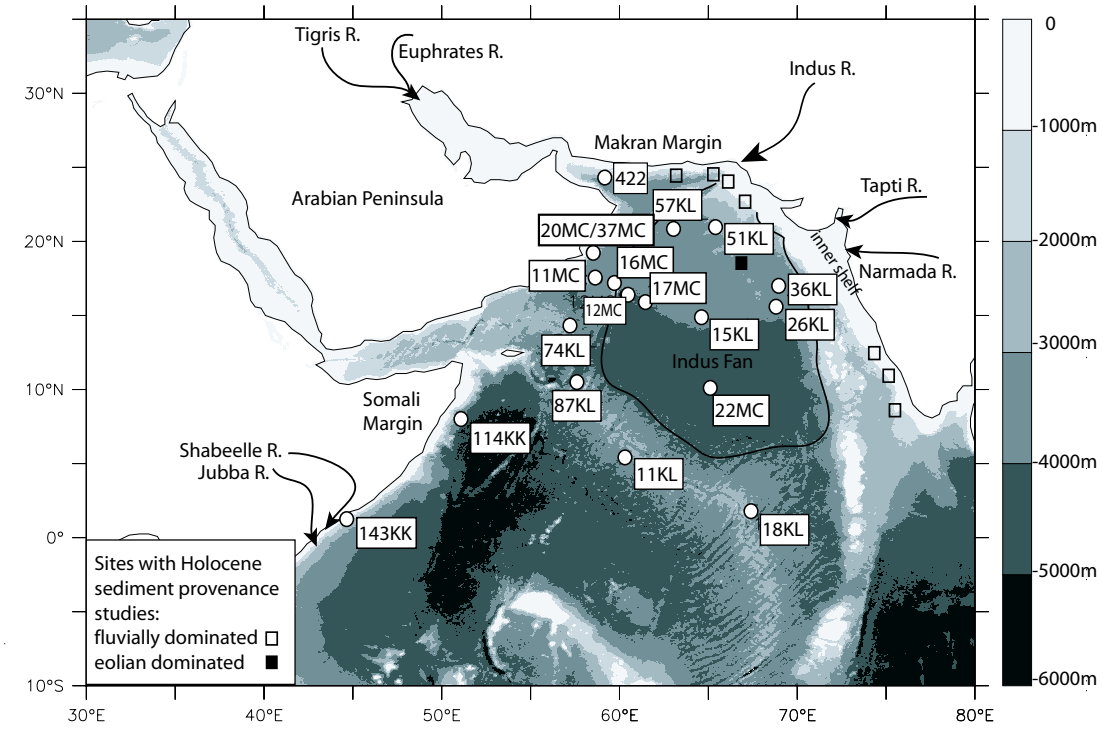

Figure 2: Map of the Arabian Sea region. Circles indicate cores used in this study. Closed square indicates a sediment core for which Holocene sedimentation is known to be predominantly eolian (Prins et al., 2000a). Open squares indicated sediment cores for which Holocene sedimentation is known to be predominantly fluvial (Sirocko and Lange, 1991; von Rad and Tahir, 1997; von Rad et al., 1999; Prins et al., 2000b; Staubwasser and Sirocko, 2001)

.

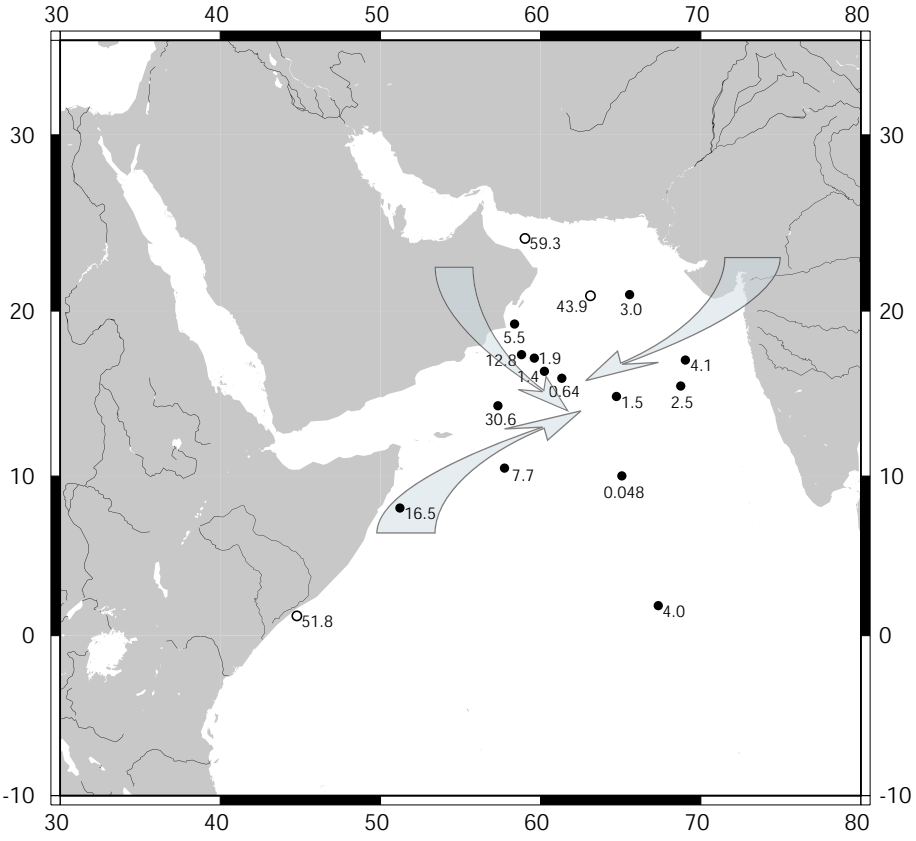

Figure 3: Leaf wax *n*–alkanoic acid (C_{24}–C_{32}) accumulation rates. Units are μg cm^{-2}kyr^{-1}. Open circles indicate sites known to be significantly affected by fluvial sedimentation (Sirocko et al., 1991). Schematic arrows are intended to highlight gradients within the data.

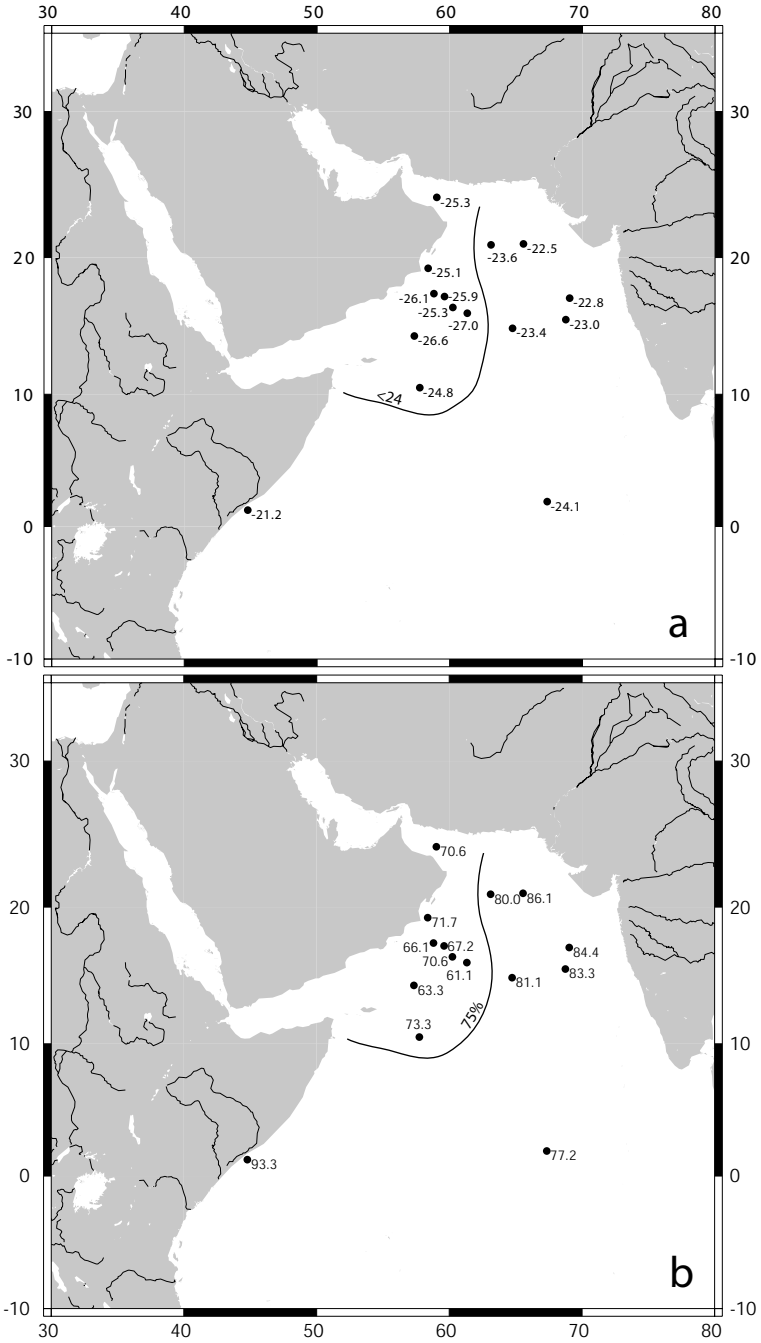

Figure 4: a) Carbon isotopic composition of C_{30} alkanoic acid. Units are permil. The isoline (hand–drawn) is intended to distinguish sites with carbon isotopic compositions of less than 24‰ from those with carbon isotopic compositions of greater than 24‰. b) Percentage of C4–derived plant waxes contributing to the total plant wax δ^{13}C in surface sediments. Percentages determined using a two end member mixing model with C_4 δ^{13}C = -20‰ and C_3 δ^{13}C = -38‰ (Chikaraishi et al., 2004). The isoline (hand–drawn) highlights sites with sites with C_4 contributions of less than 75%.

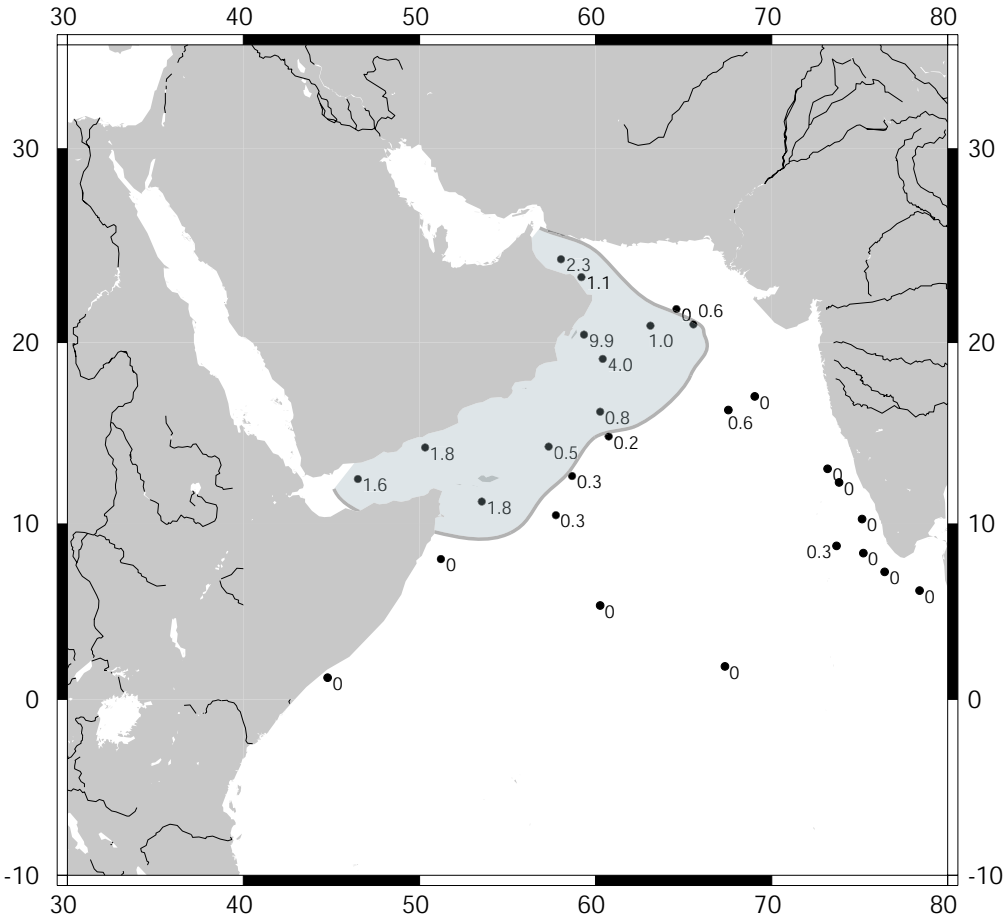

Figure 5: Dolomite accumulation rates (g $m^{-2}yr^{-1}$) from Sirocko et al. (1991). The shaded area (hand–drawn) highlights sites with dolomite accumulation rates of greater than 0.5 g $m^{-2}yr^{-1}$.

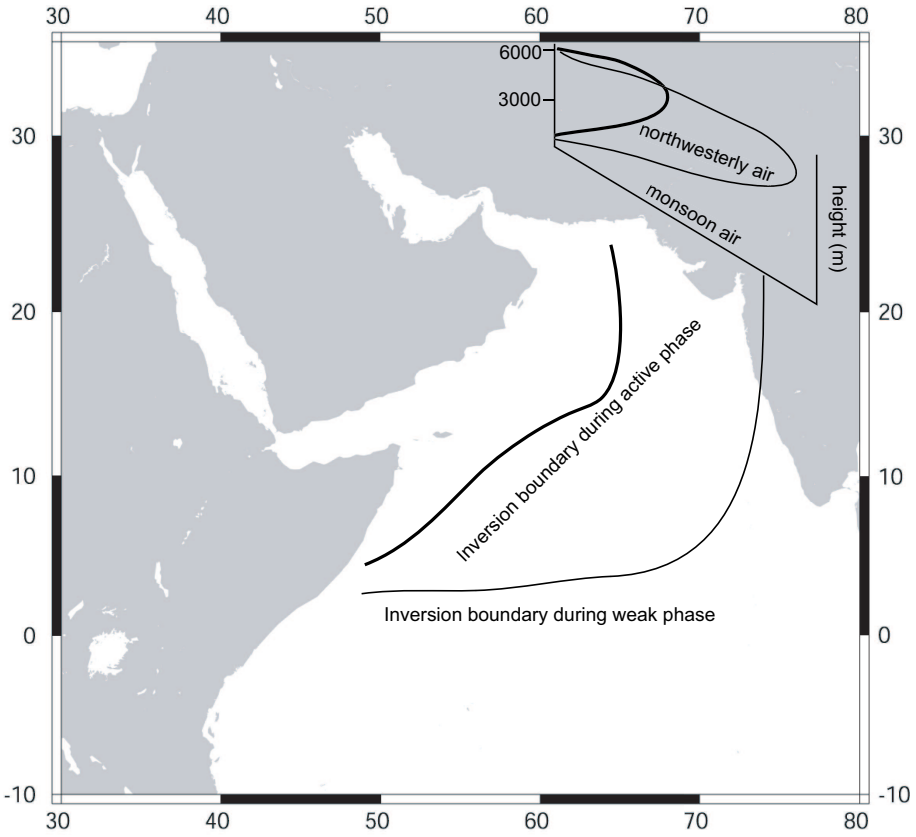

Figure 6: Schematic of the relationship between northwesterly and southwesterly winds during active (bold line) and weak (thin line) phases. Lines represent the eastward extent of the monsoon inversion. A cross section of the air masses with height in the atmosphere is also shown. Adapted from Findlater (1969) and Narayanan and Rao (1981).